https://doi.org/10.48047/AFJBS.6.3.2024.799-823

African Journal of Biological Sciences

Journal homepage: http://www.afjbs.com

Research Paper Open Access

MOLECULAR DOCKING STUDIES ON SELECTED PHYTO-COMPOUNDS IDENTIFIED FROM *Cymodocea serrulata* AGAINST HUMAN ESTROGEN RECEPTOR ALPHA (3ERT)

B.N. Poojitha[1], P. Amudha[*2], R. Vidya[2], Taslima Nasreen[1]

[1]Research Scholar, Department of Biochemistry, Vels Institute of Science, Technology and Advanced Studies, Pallavaram, Chennai - 600117, Tamilnadu, India.

[2]Assistant Professor, Department of Biochemistry, Vels Institute of Science, Technology and Advanced Studies, Pallavaram, Chennai - 600117, Tamilnadu, India.

***Corresponding Author:**Dr. P. Amudha
Assistant Professor,Department of Biochemistry,School of Life Sciences,VISTAS, Chennai-600 117.Email:amudhaa85@gmail.com,Contact No: 7904075676
Orchid ID: https://orcid.org/0000-0001-6828-9558

Article History
Volume 6, Issue 3, Mar 2024
Received:03 March 2024
Accepted :05 March 2024
Published :22 March 2024
doi:10.48047/AFJBS.6.3.2024.799-823

Abstract:
The synthesis of nanoparticles through environmentally friendly methods is a rapidly growing field within nanotechnology, known for its cost efficiency and high performance. *Cymodocea serrulate* is a seagrass that belongs to the family *Cymodoceaceae* commonly used to in traditional medicine to treat skin ailments, wounds and muscle related problems. In this study the hydroalcoholic extract of the seagrass was subjected to GC-MS analysis and anticancer effect of silver nanoparticles against MCF-7 followed by *in silico* molecular docking analysis against Estrogen receptor alpha. The study revealed the observation of twenty bioactive compounds and 14 compounds were found to possess biological activity. The *in-silico* analysis of these compounds against Estrogen receptor alpha (3ERT) showed highest binding affinity of -5.90 kcal/mol with 9,12-Octadecadienoic acid with compared to the standard doxorubicin with a binding affinity of -7.40 kcal/mol. The cytotoxic effect of the silver nanoparticles was analysed using MTT assay with MCF-7 cell line with an IC_{50} value of 102.03µg/ml and the results inferred 7.02 % cell death at 12.5 µg/ml and 79.38% cell death at 200 µg/ml while Doxorubicin inferred 87.65% at 5µg/ml. The present study provides a foundation for application of *Cymodocea serrulate* as an effective anti-cancerous agent with novel bioactive compounds for further commercialization compared to synthetic drugs available in the market for treating breast cancer.

Keywords: cytotoxicity, virtual screening, marine sources, breast cancer, anticancer

1. Introduction

Contemporary pharmaceutical science relies on natural materials obtained from cells and tissues of microbes, plants, and animals from aquatic and terrestrial environments. Natural products are secondary or specialized metabolites used in traditional medicine and are currently

considered fundamental in conventional pharmacology. Secondary metabolites are essential for enhancing competitiveness, stress tolerance, predator resistance, microbial immunity, radiation protection, and preventing biofouling in marine environments (Jin et al. 2022). Marine plants are known for their significant pharmaceutical benefits, with a long history of being utilized as traditional medicine by people for many years, marine sources have been used as anti-microbial, anti-inflammatory, anti-cancer, antifungal and antiviral agents (Kim et al. 2021). Seagrasses thrive in submerged marine environments, flourishing in tidal and subtidal regions across all sea. Seagrass biomass serves as a significant food source for coastal communities, particularly for human consumption. Seagrasses have historically been utilized in folk medicine for a wide range of therapeutic applications, such as treating fever, skin diseases, stomach problems, and as a remedy for stings from various types of rays, as well as a calming agent for infants. Seagrasses in India serve various purposes (Rengasamy et al. 2013). Utilizing bioactive compounds derived from marine sources is a common practice in the treatment of human ailments. Since its discovery, sulfated polysaccharides have been recognized as powerful chemotherapeutic or chemo preventive agents. Their anti-cancer properties have been demonstrated through boosting immunity and promoting apoptosis (Bhuyan et al. 2023). *Cymodocea serrulate* is a seagrass that belongs to the family *Cymodoceaceae* (https://www.marinespecies.org/aphia.php?p=taxdetails&id=208919) which is widely distributed in the Southwest Asian regions. The seaweeds belonging to this Genus has been traditionally used to treat skin infections, fever, muscle pain and stomach related problems (Narayanan et al. 2023). 18 million new cases were reported in 2018 (http://gco.iarc.fr/). Characteristics of tumor cells such as uncontrolled growth, the spread of disease, and metastasis are triggered by acquired genetic alterations (Senthilkumar et al. 2013). Tumor development leads to imbalanced programmed cell death, disrupted signaling pathways, angiogenesis, and weakened immune response, affecting multiple homeostatic pathways. Deregulated pathways are the primary focus of cancer treatment through chemotherapy (Atashrazm et al. 2015). This study explores the potential anticancer effects of *Cymodocea serrulate* by analyzing the phytocompounds using GC-MS, using molecular docking with Estrogen receptor alpha, and performing in vitro analysis of silver nanoparticles on a breast cancer cell line.

2. Materials and Methods

2.1 GC MS Analysis

A Shimadzu 2010 Plus system—which included a mass spectrometer, gas chromatograph, and AOC-20i auto sampler—was used to perform a thorough GC-MS analysis. A column with the parameters of 0.32 mm in diameter, 30 meters in length, and 0.50 µm in film thickness—the RTX-5Ms—was used to perform the analysis. At 70 eV, electron impact mode was the column's operating state. Maintaining an injection volume of 0.5 µL and a split ratio of 10:1 along with an injector temperature of 270 ºC ensured the best possible sample introduction. With the ion source temperature set at 200 ºC, high-purity helium gas (99.999%) was utilised as the carrier gas at a steady flow rate of 1.73 mL/min. The temperature program of the oven was thoughtfully created to efficiently separate the components of the sample. It started with

an isothermal hold of 40 ºC for two minutes, and then it increased at a rate of 8 ºC per minute to 150 ºC. The program ended with a 20-minute isothermal hold at 280 ºC. After that, the temperature was raised by 8 ºC/min to 250 ºC. 51.25 minutes was the GC's entire run time. Mass spectra covering a mass range of 40-450 Da were acquired at 70 eV with a 0.5-second scan interval during this operation. The average peak area of each component was compared to the sum of the peak areas in order to ascertain the relative share of each. The mass spectra and chromatograms generated from the analysis were processed using Turbo Mass Ver 5.2.0 software, following the methodology outlined by Srinivasan et al. (Srinivasan et al. 2013).

2.1.1. Identification of components

With the help of the National Institute of Standards and Technology's WILEY8 and FAME databases, which contain more than 65,000 patterns, the mass spectrum was analysed. The spectrums of the known components kept in the NIST08s, WILEY8, and FAME libraries were compared to the spectra of the unknown component (Dr. Dukes, 2013).

2.2 *IN VITRO* ANTI-CANCER ACTIVITY

2.2.1 Seeding and cytotoxicity Assay by Direct Microscopic observation:

MCF-7 human breast cancer cell line was obtained from the National Centre for Cell Sciences (NCCS) in Pune, India. Dulbecco's Modified Eagle Medium (DMEM) from Sigma-Aldrich in the United States was utilised for cell culture. Cells were grown in 25 cm^2 tissue culture flasks supplemented with 10% FBS, L-glutamine, sodium bicarbonate (Merck, Germany), and antibiotics to prevent contamination. Antibiotics used comprised 2.5 µg/mL of the amphotericin B, 100 µg/mL of the streptomycin, and 100 U/mL of the penicillin.

Two-day-old confluent monolayers were trypsinised and suspended in 10% growth media. A 96-well plate was seeded with 100 µL of cell suspension (5×10^3 cells per well). To ensure sterility, a 1 mg solution of AgNPs in 1 mL of DMEM was filtered using a 0.22 µm Millipore syringe filter. After 24 hours, freshly produced compounds were introduced to the growth medium, with successive dilutions (varying from 200 µg/mL to 12.5 µg/mL) in 5% DMEM. Each concentration was added to the wells three times, and the cells were cultured for twenty-four hours. Doxorubicin (5 µg/mL) was used as the standard medication, with untreated cells acting as controls. After the treatment period, cell morphology changes, including granulation, rounding, shrinkage, or cytoplasmic vacuolization, were observed using an Olympus CKX41 inverted phase-contrast microscope equipped with an Optika Pro5 CCD camera, indicating cytotoxicity

2.2.2 Cytotoxicity Assay by MTT Method:

To perform the MTT assay, 15 milligrammes of MTT (Sigma, M-5655) were dissolved in three millilitres of phosphate-buffered saline (PBS) to form a concentrated MTT solution. The fluid was then filtered to assure sterility. After a 24-hour incubation, 30 µL of reconstituted MTT solution was applied to each well of the 96-well plate, containing both test and control samples, after removing the old culture medium. The plate was put in a humidified 5% CO2 incubator at 37ºC and incubated for 4 hours with moderate shaking to allow the MTT to be metabolised by live cells to generate formazan crystals. Following the incubation period, the media was carefully taken out of each well and the formazan crystals were dissolved with the addition of 100 µL of MTT Solubilisation Solution (dimethyl sulfoxide, DMSO; Sigma-

Aldrich, USA). A gentle up-and-down pipetting motion was used to guarantee total dissolution.
.
% Cytotoxicity using the following formulas:
% Cytotoxicity = 100 - [Abs (Test) /Abs (control)] x100.
% Cell Viability = [Abs (Test) /Abs (control)] x100.

2.3 Statistical analysis

The IC50, or the amount of AgNPs required to suppress the growth of cancer by 50%, was visually estimated using a linear regression approach using the graphpad Instat (version 3) program, which is based on Microsoft Windows. Graphics were used to express the results.

2.4 *IN SILICO* MOLECULAR DOCKING

2.4.1 Ligand and protein preparation

Molecular modelling has been successfully applied with a variety of software applications that are based on algorithms in pharmaceutical research recently, thanks to computational drug discovery methodologies. By using these programs to compute ligand and protein binding scores, researchers can choose the best software for protein-ligand interactions and get the best possible outcomes (Velavan et al., 2020).
The PubChem database provided the ligands employed in this investigation, and the standard drug doxorubicin. Open Babel was used to translate these ligands into PDB format. The Protein Data Bank (PDB) provided the human oestrogen receptor alpha (PDB ID: 3ERT). Using PyMOL software, the protein was prepped before docking by eliminating all ligand molecules and water molecules. The protein was then stored in PDB format.

2.4.2 *In Silico* Docking Studies

Protein Data Bank (PDB), a protein databank was utilised to obtain the structures of the protein, and PubChem was used to obtain ligands. Grids, docking scores, and conformers of activators attached to the protein's active site were all produced using AutoDock Tools, which also offers an automated docking interface. ACD/ChemSketch was utilised to minimise energy, and the minimised structures were then employed for docking investigations. Heteroatoms like water molecules and other superfluous atoms were eliminated from the protein structures in order to make them ready for docking. The Lamarckian genetic method, which was included in AutoDock 4.1, was used in the docking procedure. This program determines the ideal flexible ligand position with the lowest energy by estimating interaction energies. All torsions are allowed to rotate since the scoring function assesses the intermolecular interactions that occur between the protein and the ligand during docking. The parameters of the grid map were set at centre x = 24.20, centre y = 5.57, and centre z = 22.15, with the focus being on certain protein residues. Following default parameters, minimisation was performed using the pseudo-Solis and Wets methods and the Lamarckian genetic algorithm (Ghose and Crippen, 1987; Binkowski et al., 2007; Vidya et al., 2012; Shruthi et al., 2012). Modelling software such as PyMOL (version 1.1, Delano Scientific LLC, San Carlos, CA, USA), Chimaera (version 1.10.1, UCSF Resources for Biocomputing, Visualisation, and Informatics, NIH, CA, USA), and PoseView (Trot and Olson, 2010) were used to visualise the complicated structures.

3. RESULTS

3.1 Identification of bioactive compounds in hydroalcoholic extract by GC MS analysis

The hydroalcoholic extract was analysed using GC-MS and twenty components were found. Table 1 and Figure 1 depicts the chromatogram of the extract obtained from the GC-MS analysis. The main chemicals discovered were n-Hexadecanoic acid, n-Nonadecanol-1, 2-Hexadecen-1-ol, 3,7,11,15-Tetramethyl, 9,12-Octadecadienoic acid, 9,12,15-Octadecatrienoic acid, Octadecanoic acid, and Octadecanoic acid ethyl ester. The existence of these many bioactive chemicals supports the plant's traditional usage in treating a variety of diseases. Further separation of individual phytochemical elements and study of their biological activity (as indicated in Table 2) is expected to generate useful results.

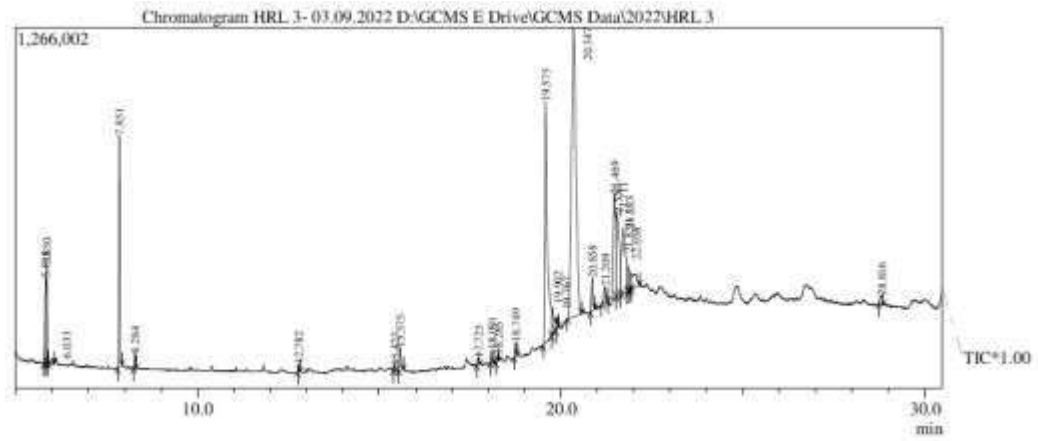

Figure 1: Chromatogram of hydroalcoholic extract

Peak#	R.Time	I.Time	F.Time	Area%	Height%	A/H	Mark	Name
1	5.818	5.775	5.833	2.58	5.91	2.03		Butane, 1,1 diethoxy-3-methyl
2	5.85	5.833	5.9	2.53	6.82	1.72	V	Pentane, 1,1-diethoxy
3	6.033	5.9	6.058	0.11	0.36	1.49	V	3,3-DIETHOXY-2-BUTANONE
4	7.851	7.8	7.933	6.93	16.07	2		Propane, 1,1,3 -triethoxy
5	8.284	8.25	8.333	0.44	1.05	1.94		1,1,3-TRIETHOXYBUTANE
6	12.782	12.75	12.825	0.24	0.54	2.02		Undecane, 3,8-dimethyl
7	15.423	15.392	15.458	0.15	0.35	2.03		Dodecane, 1-iodo
8	15.575	15.525	15.658	1.03	1.58	3.03		1,2 -BENZENEDICARBOXYLIC ACID,DIE
9	17.725	17.683	17.758	0.25	0.49	2.4		Octadecanoic acid,2-oxo-,methyl ester
10	18.091	18.05	18.142	0.45	0.94	2.2		Isopropyl myristate
11	18.265	18.2	18.292	0.21	0.48	2.07		2,6,10-TRIMETHYL, 14-ETHYLENE-14-PENTADECENE
12	18.749	18.708	18.8	0.57	1.04	2.54		8-Hexadecenal, 14-methyl-,(Z)
13	19.575	19.508	19.742	16.98	16.72	4.72		n-Hexadecanoic acid
14	19.767	19.742	19.858	1.71	1.77	4.5	V	Phthalic acid, ethyl pentyl ester
15	19.902	19.858	19.95	0.6	0.81	3.47	V	ETHYL PENTADECANOATE
16	20.347	20.183	20.567	36.59	20	8.5		Dotriacontane n-Dotriacontane Bicetyl
17	20.858	20.808	20.925	1.44	2.29	2.91		n-Nonadecanol-1
18	21.209	21.125	21.267	0.91	1.11	3.81		2-HEXADECEN-1-OL,3,7,11,15-TETRAMETHYL
19	21.469	21.267	21.525	7.97	7.14	5.18	V	9,12-Octadecadienoic acid (Z,Z)
20	21.55	21.525	21.658	7.04	5.42	6.03	V	9,12-Octadecadienoic acid (Z,Z,Z)
21	21.711	21.658	21.833	6.86	4.48	7.11	V	Octadecanoic acid
22	21.85	21.833	21.875	0.82	1.65	2.3	V	Benzothiophere-3-carboxylic acid, 4,5,6,7-tetra
23	21.883	21.875	21.942	0.94	1.39	3.15	V	Phosphoramidous dibromide, dimethyl-
24	22.058	21.942	22.158	1.94	0.94	9.55	V	OCTADECANOIC ACID,ETHYL ESTER
25	28.816	28.733	28.867	0.71	0.65	5.09		1,2-BENZENEDICARBOXYLIC ACID
				100	100			

Table 1: Identification of bioactive compounds in hydroalcoholic extract by GC MS analysis

Table 2 Biological activity of compounds identified in hydroalcoholic extract using GC-MS

Peak	R. Time	Name of the compounds	Biological activity**
1	19.57	n-Hexadecanoic acid	Antioxidant, Hypocholesterolemic, Nematicidal, Pesticidal, Hemolytic, Antiandrogenic, Hemolytic, 5-Alpha Reductase Inhibitor
2	20.85	n-Nonadecanol-1	Antioxidant, Antibacterial, Antimicrobial, Cytotoxic effect, Antimicrobial Antimalarial, Anti HIV, Unini uses like weakness of the principal organs like heart, Brain, liver, General weakness, Haemoptysis, Palpitation, Conjunctivitis, Earache, Stomatitis
3	2021	2-hexadecen-1-ol, 3,7,11,15-tetramethy	Antimicrobial, Cancer-preventive, Anti-inflammatory, Analgesic, Fungicide activity
4	21.46	9,12-Octadecadienoic acid	Anti-inflammatory, Hypocholesterolemic Cancer preventive, hepatoprotective, nematicide, insectifuge, antihistaminic antieczemic, anticancer, 5-Alpha reeducates inhibitor, anti-androgenic, Anti-arthritic, anti-coronary.
5	21.55	9,12,15-Octadecatrienoic acid	Arachidonic acid-Inhibitor, Increase Aromatic Amino Acid Decarboxylase Activity, Inhibit Production of Uric acid.
6	21.17	Octadecanoic acid	Antioxidant and anti-inflammatory
7	22.05	Octadecanoic Acid, ethyl ester	Anti-inflammatory, antiandrogenic, cancer preventive, dermatitigenic activity

**Source: Dr. Duke's phytochemical and ethnobotanical databases [Online database].

3.2 *In vitro* anti-cancer activity of AgNPs in Human breast cancer cell line (MCF-7)

The study assessed the reduction of cell growth in the MCF-7 cell line by silver nanoparticles (AgNPs) at different concentrations (12.5, 25, 50, 100, and 200 µg/mL). The findings revealed a favourable association between AgNP concentration and cell growth inhibition. The lowest inhibition was reported at 7.02% for the 12.5 µg/mL concentration, demonstrating limited action at lower dosage. The maximum inhibition was 79.38% at 200 µg/mL, indicating a strong impact on cell growth at higher dosages. In comparison, the conventional treatment Doxorubicin at 5 µg/mL inhibited growth by 87.65%, higher than that achieved with AgNPs. Figure 2 depicts the dose-dependent increase in cell growth inhibition with increasing AgNP concentrations. Figure 3 depicts the cell viability percentages for MCF-7 cells treated with AgNPs, demonstrating a gradual fall in viability as the AgNP concentration rose.

Table 3 and Figure 4 demonstrate that the IC50 value (concentration of AgNPs necessary to inhibit 50% of cell growth) is 102.03 µg/mL. This value represents the potency of AgNPs in inhibiting MCF-7 cell growth. Figure 5 depicts the morphological alterations observed in MCF-7 cells following exposure to various doses of AgNPs. Notable modifications include changes in cell shape and size, as well as the presence of cell damage markers, demonstrating AgNPs' cytotoxic effects on the MCF-7 cell line. These data indicate that AgNPs impede cell development in a concentration-dependent manner and generate major morphological alterations in cancer cells.

Table 3 Cell growth inhibition and cytotoxicity of AgNPs on MCF 7cell line by MTT assay

S.No.	Concentrations (µg/ml)	Absorbance (Optical density)	Cell growth inhibition (%)	Cell Viability (%)
1	12.5	0.775	**7.02**	92.98
2	25	0.713	14.51	85.49
3	50	0.537	35.56	64.44
4	100	0.283	66.01	33.99
5	200	0.172	**79.38**	20.62
Standard (Doxorubicin) (5µg/ml)		0.103	87.65	12.35

Cell Control	0.834	100	0
Half Inhibition Concentration (IC_{50})			**102.03µg/ml**

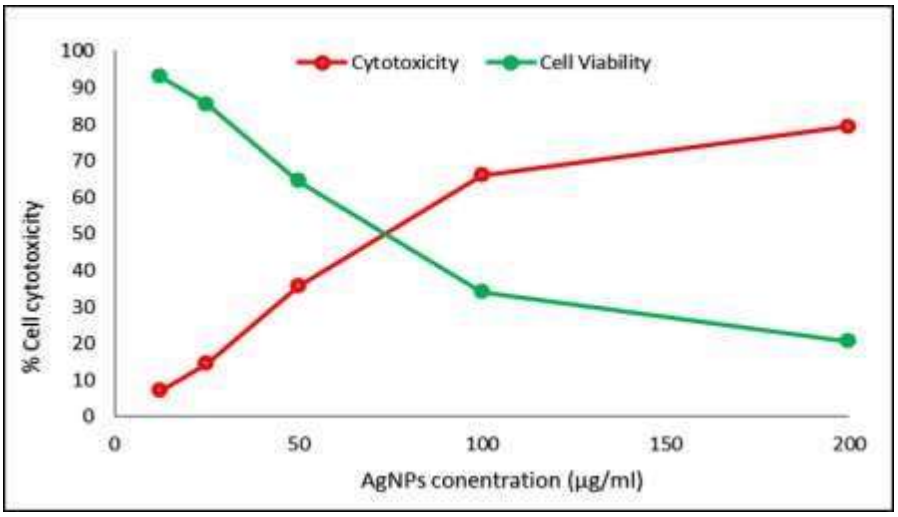

Figure 2: Percentage of cell growth inhibition of AgNPs on MCF 7cell line by MTT assay

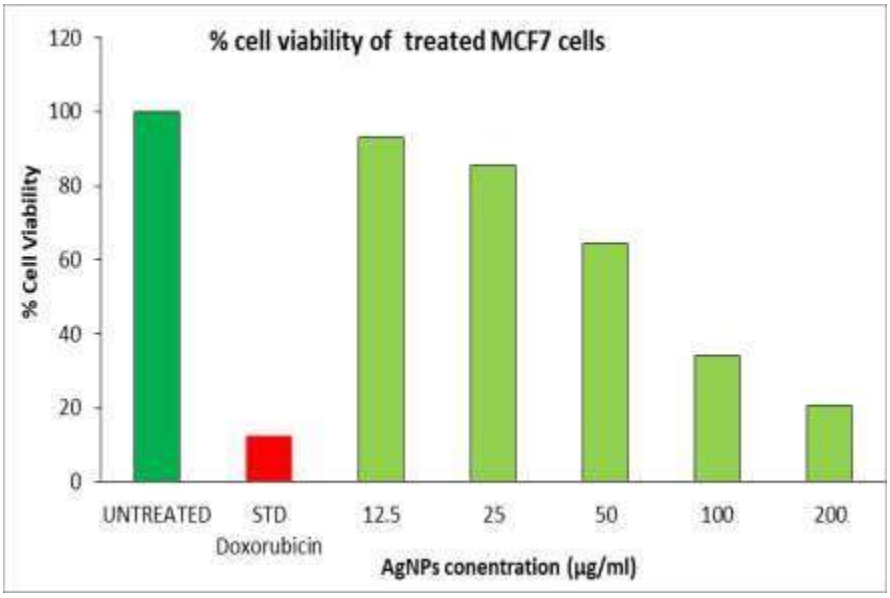

Figure 3: Cell viability percentage of AgNPs treated MCF-7 cells.

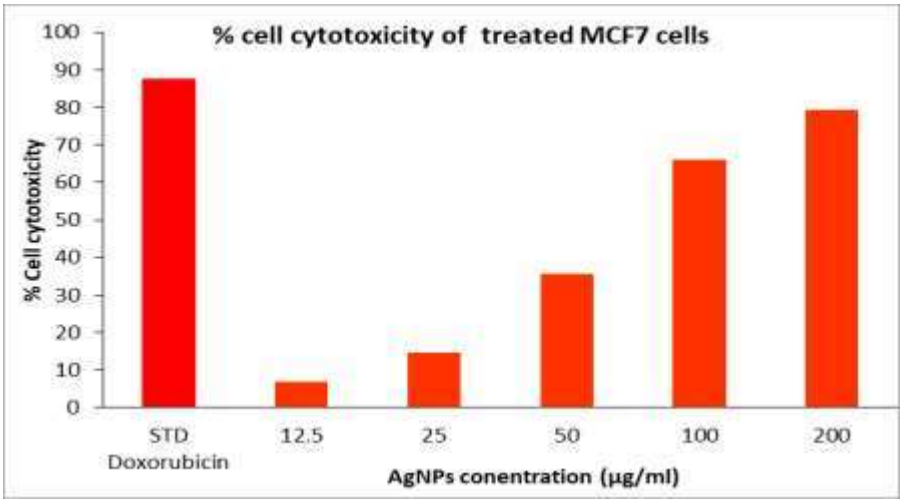

Figure 4: Cytotoxicity of cells treated with AgNPs on MCF-7 cells.

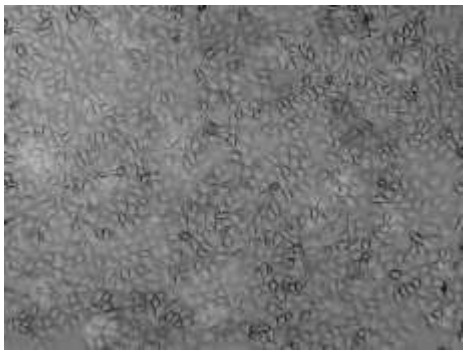

Control

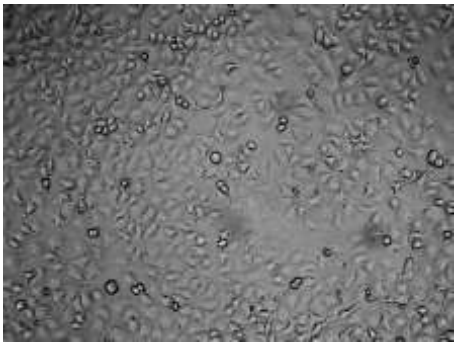

12.5µg/ml

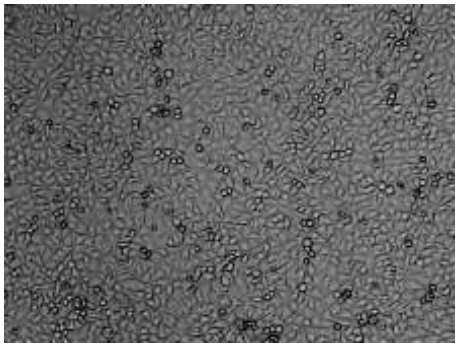

25µg/ml

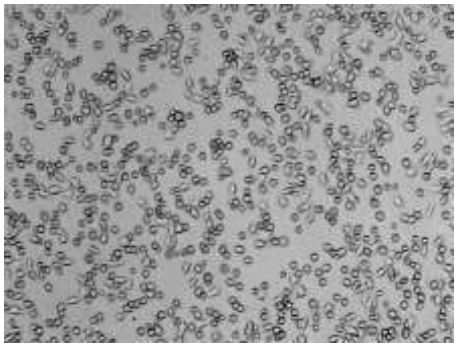

50 µg/ml

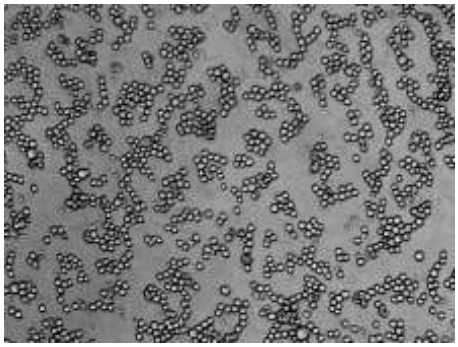

100µg/ml

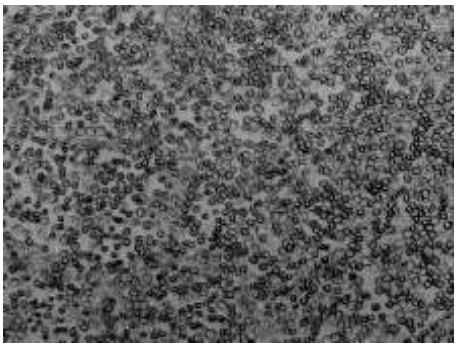

200µg/ml

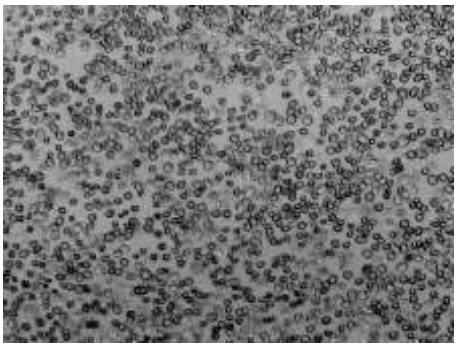

Standard (Doxorubicin)

Figure 5: Photomicrograph of MCF-7 cell line on different concentrations of AgNPs treatment

3.3 *Insilico* Studies

According to Atkovska et al. (2014), in silico molecular docking studies have become indispensable instruments in contemporary drug discovery, providing a dependable way to pinpoint active sites on target receptors, examine the interactions that compounds have when they bind to proteins, and forecast the properties of different molecules that make them suitable as drugs (Atkovska et al., 2014). The assessment of ligand-receptor binding efficiency is a critical task for these investigations, as it provides insight into the possible therapeutic benefits of candidate drugs (Mooers, 2020). The involvement of oestrogen in the development of breast cancer is one important field of investigation. One well-established element in the development and course of breast cancer is oestrogen hyperproduction. The two primary types of oestrogen receptors found in the human body are ER-α and ER-β. Specifically, the uterus and mammary glands express ER-α the most. Increased production and proliferation of ER-α in mammalian cells can result from overactivity of oestrogen, and this is intimately associated with the growth and maintenance of several forms of breast cancer (Sahayarayan et al., 2021). For the purpose of researching cancer drugs, ER-α becomes a crucial molecular target.

The purpose of this study is to investigate the potential of a number of bioactive substances that have been isolated from the plant Cymodocea serrulate, such as, 2-hexadecen-

1-ol, n-Nonadecanol-1, Octadecanoic acid ethyl ester, 3,7,11,15-Tetramethyl, n-Hexadecanoic acid and 9,12-Octadecadienoic acid. With an eye towards their potential as anticancer medicines, we examine their interactions with the human oestrogen receptor alpha (PDB ID: 3ERT). In order to evaluate these compounds' potential for use in cancer therapy, their efficacy will be compared to that of the widely used medication doxorubicin. With this strategy, we hope to learn more about how to use natural substances to treat cancer and potentially identify new therapeutic avenues.

n-Nonadecanol-1
(6a)

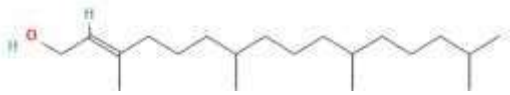

2-hexadecen-1-ol, 3,7,11,15-Tetramethyl
(6b)

9,12-Octadecadienoic acid
(6c)

n-Hexadecenoic acid
(6d)

Octadecanoic acid, ethyl ester
(6e)

Doxorubicin
(6f)

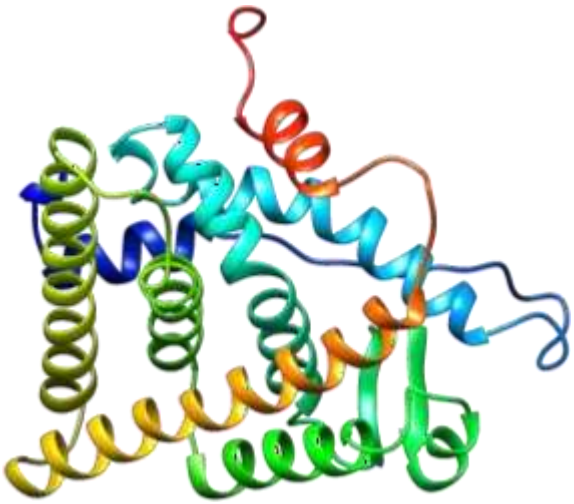

Human estrogen receptor alpha (PDB ID: 3ERT)
(6g)
Figure 6a-6f: 2D view of selected ligand and (6g) 3D view of target protein

In order to assess the binding affinity of particular bioactive substances with the human oestrogen receptor alpha (3ERT), this study employed comprehensive molecular docking analyses. Both 2D and 3D visualisations were used to study the structures of the ligands and the target protein. The 2D images of the chosen ligands, which shed light on their molecular interactions and structures, are shown in Figures 6a through 6f. The target protein's three-dimensional view is shown in Figure 6g, which provides a thorough comprehension of the receptor's spatial structure.Stronger binding affinities are indicated by more negative docking scores, and this information is essential for locating drugs that interact with target proteins more effectively. Based on their docking energy and advantageous interactions with the target protein's active site residues, the ligands were chosen for docking. **Table 4** provides an overview of the docking studies' findings and details the interactions and binding energies of the docked ligand molecules. For every ligand, the docking interactions are shown in detail in Figures 7a through 12b. n-Hexadecanoic acid (-5.60 kcal/mol), 2-hexadecen-1-ol, 3,7,11,15-Tetramethyl (-4.90 kcal/mol), 9,12-Octadecadienoic acid (-5.90 kcal/mol), n-Nonadecanol-1 (-5.50 kcal/mol), Octadecanoic acid ethyl ester (-5.40 kcal/mol), and Doxorubicin (used as a standard reference, -7.40 kcal/mol) are the specific compounds analysed in these figures. Hydrogen bonding and hydrophobic interactions were the main characteristics of the binding interactions between these ligands and the target protein.

Through their binding interactions, the chemicals that were selected for docking studies demonstrated considerable anticancer activity, with the ability to block the Human Oestrogen Receptor Alpha. 9,12-Octadecadienoic acid showed the strongest action of all the chemicals examined; it was followed by n-Hexadecanoic acid, n-Nonadecanol-1, Octadecanoic acid ethyl ester, 2-hexadecen-1-ol, and 3,7,11,15-Tetramethyl. These results imply that these bioactive substances, especially those that target the human oestrogen receptor alpha, may make good candidates for additional research and development as anticancer treatments.

Table 4: Molecular docking of Human estrogen receptor alpha (PDB ID: 3ERT)

Ligand	Molecular formula	M. weight (g/mol)	H-bond donors / acceptors	Binding Affinity (kcal/mol)	Ligand binding site of target (Protein ID: 3ERT) Amino acids
n-Hexadecanoic acid	$C_{16}H_{32}O_2$	256.42	1/2	-5.60	**Trp 383**, Met 343, Leu 525, Leu 428, Met 421, Ile 424, Leu 346, Met 388, Leu 391, Leu 387, Phe 404, Leu 384, Ala 350, Leu 349, Arg 394, Glu 353.
2-hexadecen-1-OL, 3,7,11,15-Tetramethyl	$C_{20}H_{40}O$	296.50	1/1	-4.90	Leu 354, Leu 536, Val 533, Asp 351, **Trp 383**, Thr 347, Met 528, Cys 530, Leu 525, Lys 529, Tyr 526.
9,12-Octadecadienoic acid	$C_{18}H_{32}O_2$	280.40	1/2	-5.90	Arg 39, Leu 428, Ile 424, Ala 350, Asp 351, Leu 525, **Trp 383**, Met 388, Leu 384, Leu 349, Leu 391, Leu 346, Met 421, Leu 387, Glu 353, Thr 347, Met 343, Phe 404.
n-Nonadecanol-1	$C_{19}H_{40}O$	284.50	1/1	-5.50	Gly 521, Ile 424, Thr 347, Met 528, Leu 525, Met 421, **Trp 383**, Ala 350, Leu 346, Leu 384, Arg 394, Leu 391, Leu 387, Phe 404, Met 388, Leu 428, Leu 349.
Octadecanoic acid ethyl ester	$C_{20}H_{40}O_2$	312.50	0/2	-5.40	Leu 354, Leu 387, Leu 391, Phe 404, Ile 424, Leu 346, Met 343, Met 421, Ala 350, Gly 521, Leu 384, Leu 525, Thr 347, **Trp 383**, Leu 536.
*Doxorubicin (Std.)	$C_{27}H_{29}NO_{11}$	543.50	6/12	-7.40	Asp 351, Leu 354, Ala 350, **Trp 383**, Leu 536, Met 522, Tyr 526, Lys 531, Cys 530, Pro 535, Leu 539, Val 534, Val 533.

* Trp 383 amino acid residues were involved in all selected ligand-binding interactions.

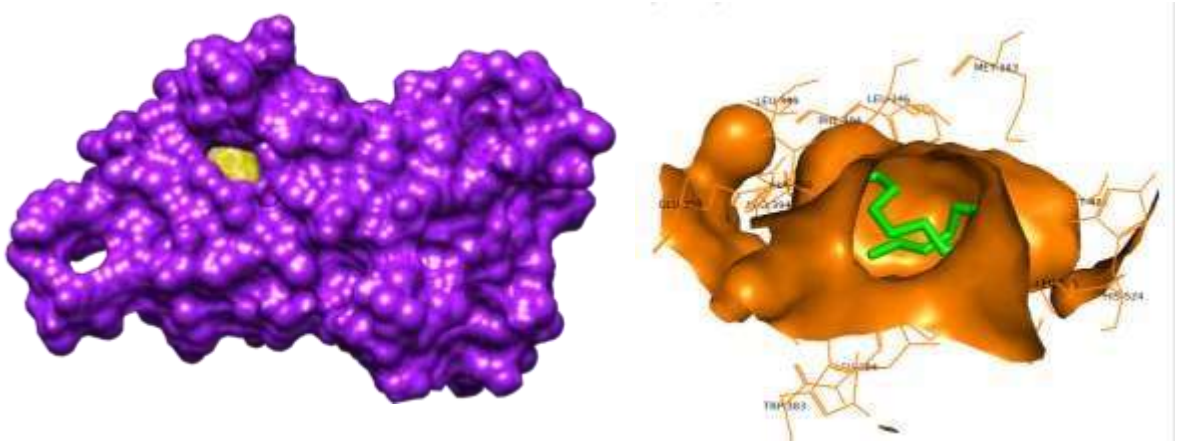

Docked complex **Ligand binding site**

Figure 7a: 3D surface view of Human estrogen receptor alpha complex with n-Hexadecanoic acid

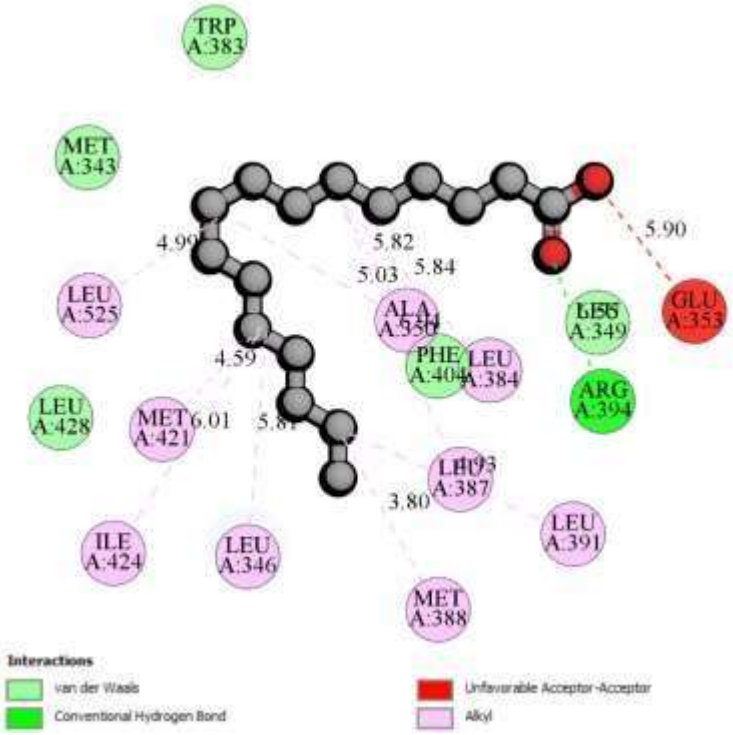

Figure 7b: 2D view of n-Hexadecanoic acid interaction with Human estrogen receptor alpha amino acid residues

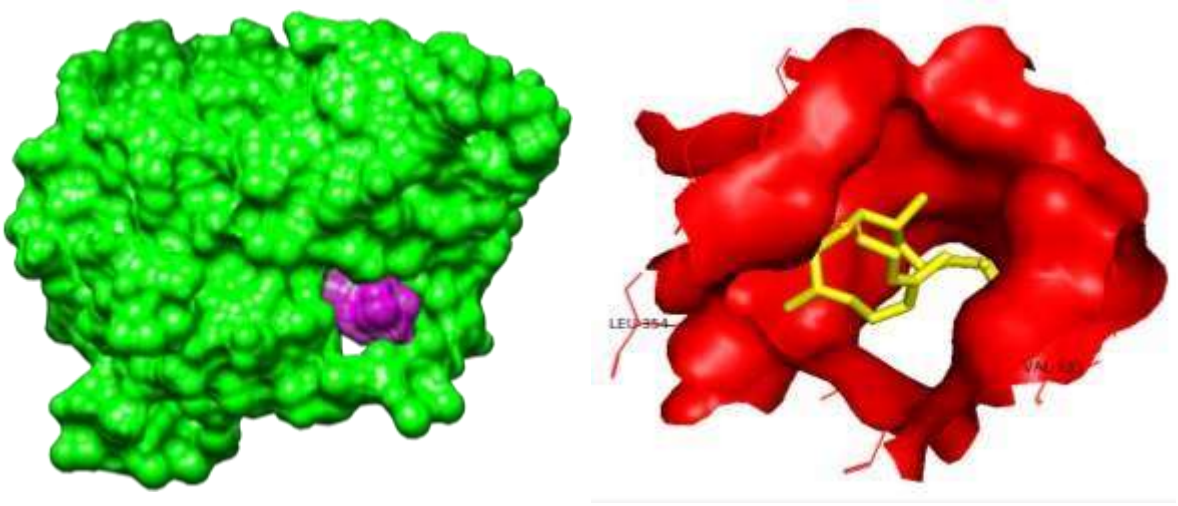

Docked complex **Ligand binding site**

Figure 8a: 3D surface view of Human estrogen receptor alpha complex with 2-hexadecen-1-OL, 3,7,11,15-Tetramethyl

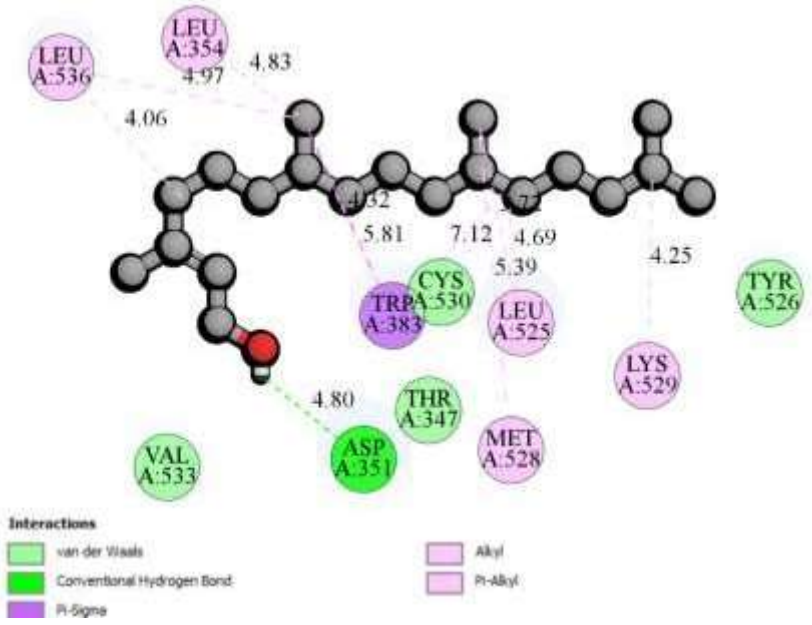

Figure 8b: 2D view of 2-hexadecen-1-OL, 3,7,11,15-Tetramethyl interaction with Human estrogen receptor alpha amino acid residues

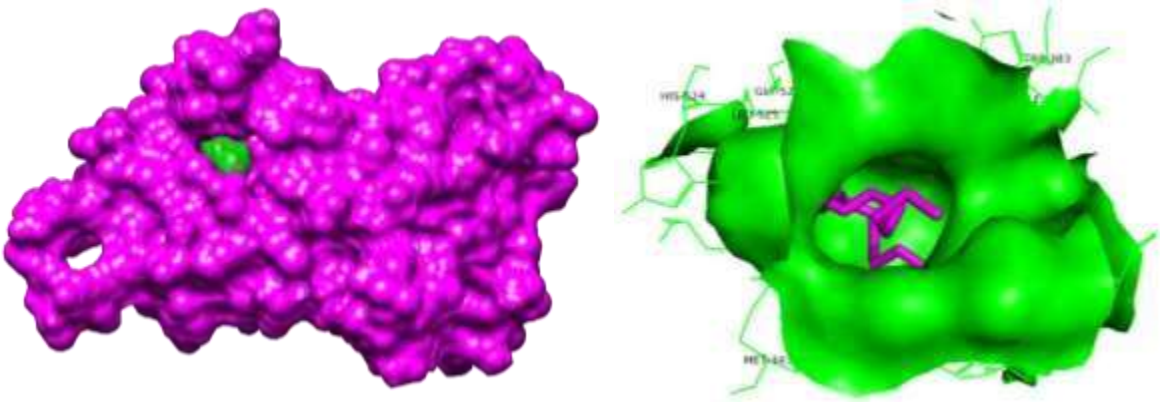

Docked complex **Ligand binding site**

Figure 9a: 3D surface view of Human estrogen receptor alpha complex with 9,12-Octadecadienoic acid

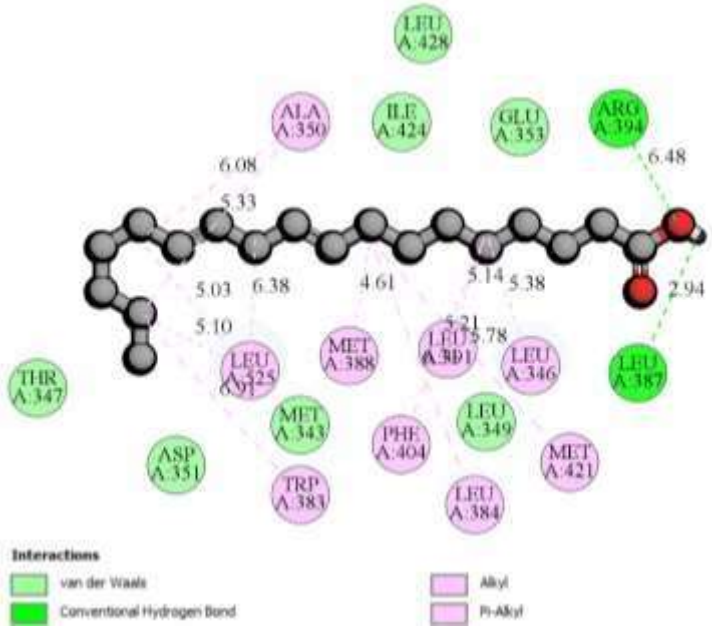

Figure 9b: 2D view of 9,12-Octadecadienoic acid interaction with Human estrogen receptor amino acid residues

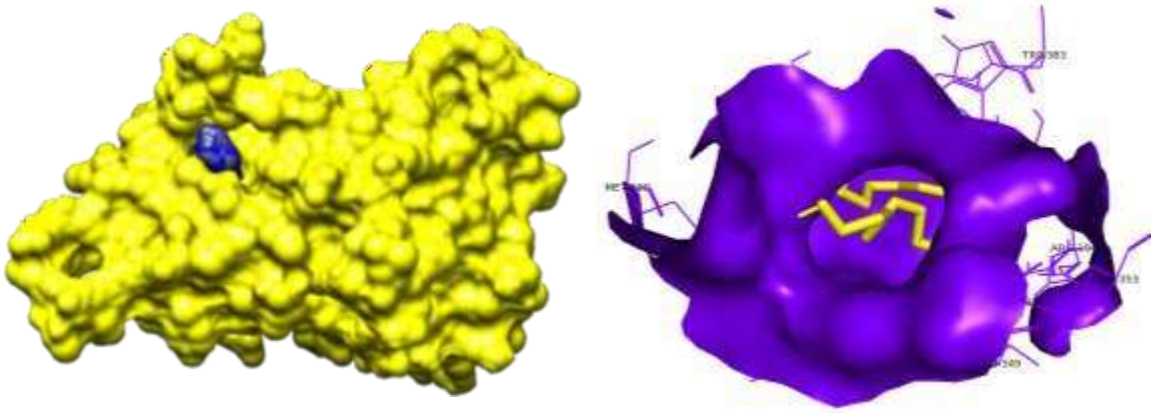

Docked complex **Ligand binding site**

Figure 10a: 3D surface view of Human estrogen receptor alpha complex with n-Nonadecanol-1

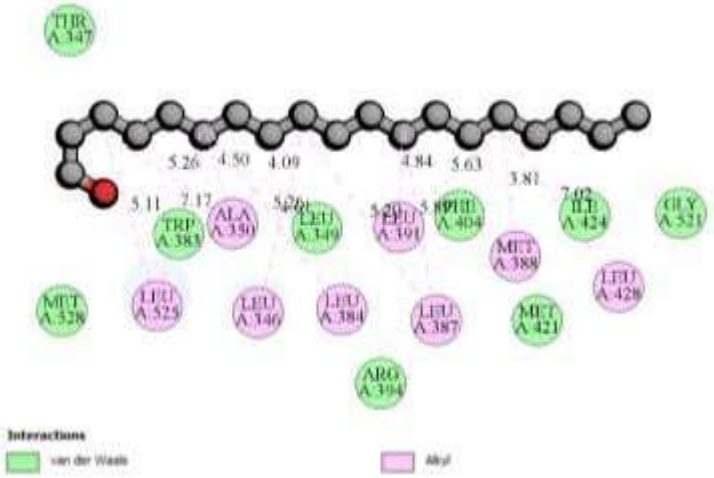

Figure 10b: 2D view of n-Nonadecanol-1 interaction with Human estrogen receptor amino acid residues

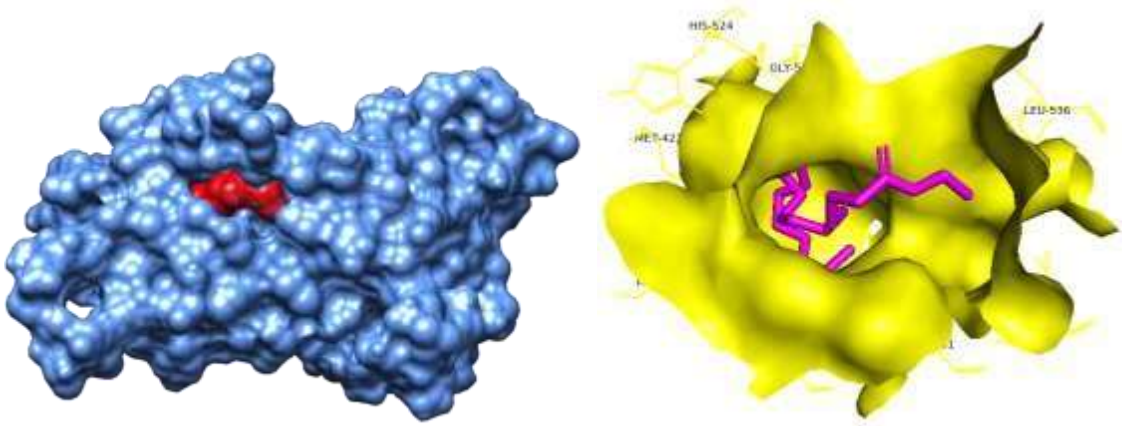

Docked complex **Ligand binding site**

Figure 11a: 3D surface view of Human estrogen receptor alpha complex with Octadecanoic acid, ethyl ester

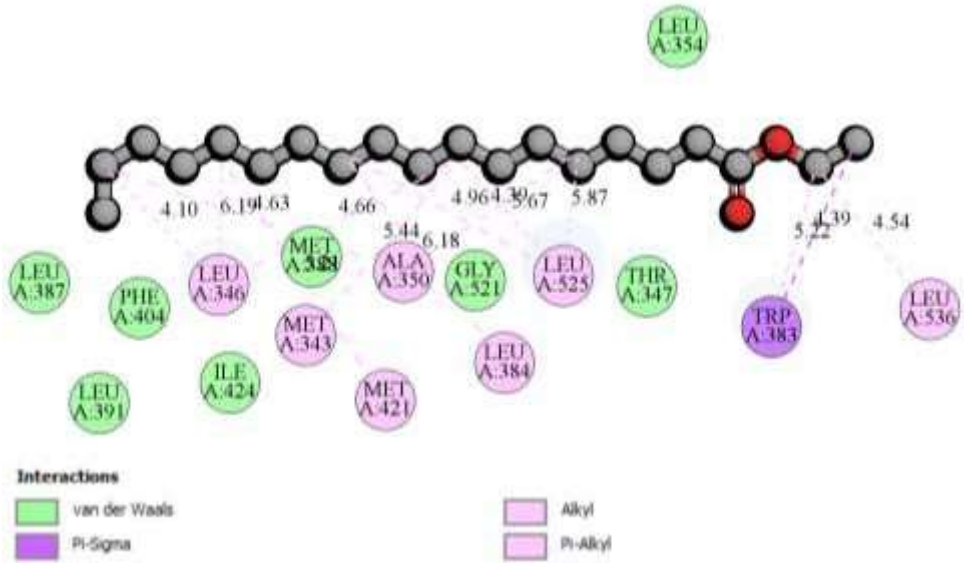

Figure 11b: 2D view of Octadecanoic acid, ethyl ester interaction with Human estrogen receptor amino acid residues

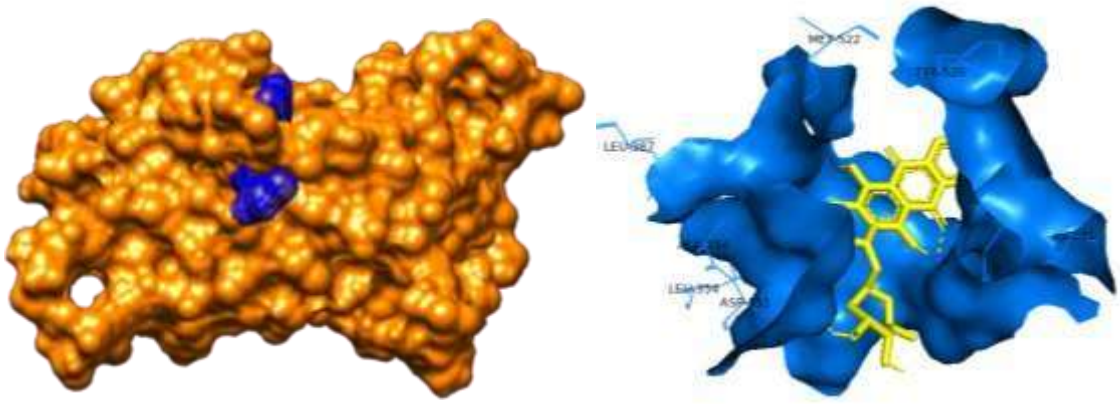

Docked complex **Ligand binding site**

Figure 12a: 3D surface view of Human estrogen receptor alpha complex with Doxorubicin

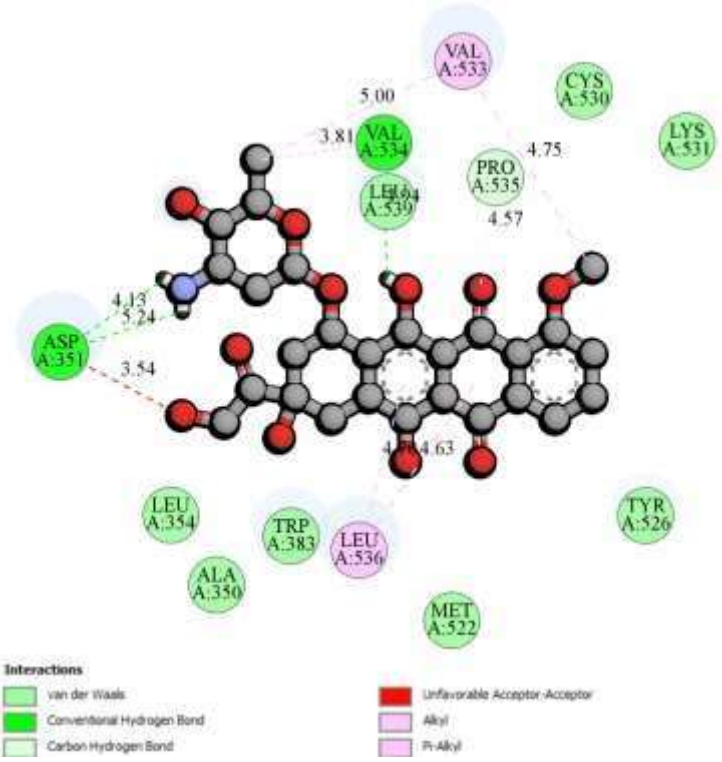

Figure 12b: 2D view of Doxorubicin interaction with Human estrogen receptor amino acid residues

Discussion

Gas chromatography (GC) and mass spectrometry (MS) are combined to identify distinct compounds in a mixture. This was the initial integration of a separation technology with a spectrometry approach to swiftly analyse chemical components. GC-MS is a highly potent, versatile, and commonly utilized method for examining chemical combinations in

various fields such as drug screening, forensic investigations, environmental studies, trace analysis.

The GC-MS analysis of the hydroalcoholic extract of *Cymodocea serrulata* revealed the presence of twenty compounds of which fatty acid and its esters were more predominantly present. The ethyl acetate extract of *Cymodocea serrulate* was found to exhibit antimicrobial activity against the *E. coli*, *B. subtilis and C. pneumoniae* and their GC-MS analysis revealed the presence of 14 major phytocompounds that were pharmaceutically valuable (Narayanan et al. 2023). In a similar study, the GC-MS analysis of n-hexane:ethyl acetate of *Cymodocea serrulate* revealed the presence of 104 bioactive compounds including tetradecane, dodecanal, phytol, butanoic acid, stigmasterol, hexadecenoic acid and benzene(Das et al. 2023). Another marine algae *Acoathophora deilei* revealed the inclusion of methyl ester, 9-octadeconic acid, dibutyl phthalate and 1,2- benzendicarboxylic acid (Datchanamurthy et al. 2022). Further analysis was carried out with silver nanoparticle to study the cytotoxic effect (MCF-7) using formazan production, after the addition of MTT stain on the pre-incubated cells in 96-well plate, indicated higher cytotoxic effect(Nadar Rajivgandhi et al. 2022).

To study the anticancer activity of silver nanoparticles against breast cancer cell line MCF-7 cell line was used at concentrations ranging from 12.5-200μg/ml and the IC_{50} of AgNPs was obtained at102 μg/ml and cell growth inhibition was found to be highest at 200 μg/ml with an inhibition percentage of 79.38 and standard doxorubicin showed a inhibition of 87.65% at 5 μg/ml. in a similar study the cytotoxicity of *Cymodocea serrulate* AgNPs was found to be 34.5 μg/ml on HeLa cells (Chanthini et al. 2015).

Estrogen levels have been linked to the development of osteoporosis, breast cancer, and uterine cancer Estrogen receptor (ER) is present in various tissues such as the endometrium, breast cancer, and ovarian stromal cells, as well as the hypothalamus, where it stimulates cell proliferation (Bray et al. 2018) (Levin 2005). The active metabolite of Tamoxifen is 4-hydroxytamoxifen (4-OHT) (Sanyakamdhorn et al. 2016). Tamoxifen is a commonly prescribed antiestrogen adjuvant medication for ER-positive breast cancer women. Tamoxifen is frequently utilized in the treatment of postmenopausal women with ER+ malignancies. Moreover, the ER complex bound to tamoxifen inhibits the activation of genes by estrogen, thereby blocking the cancer cell growth caused by estrogenic actions (Chang 2012). Molecular docking analysis of the compounds from the hydroethanolic extract of *C. serrulate* against estrogen receptor alpha with standard drug doxorubicin revealed that 9,12-Octadecadienoic acid has potential activity followed by n-Hexadecanoic acid, n-Nonadecanol-1, Octadecanoic acid ethyl ester and n2-hexadecen-1-pl, 3,7,11,15-Tetramethyl with a binding affinity of -5.90, -5.60, -5.50, -5.40 and -4.90 kcal/mol respectively. The standard drug Doxorubicin exhibited binding affinity of -7.40 kcal/mol. The compound n-Hexadecanoic acid contain two conventional hydrogen bonds with ARG 394 ana LEU 387 and Van der Waals bonds with amino acid residues LEU 428, ILE 424, GLU 353, THR 347, ASP 351, MET 343 and LEU 349. In a similar study bioactive compounds identified from *Caulerpa racemose* were subjected to in silico analysis against ER alpha receptor and a standard drug mitoxantrone. The study revealed that caulerpin exhibited potential anticancer activity compared to other compounds with a highest binding affinity of -11.8 kcal/mol and the standard with -8.45

kcal/mol, the compound was found to exhibit strong hydrogen bond with HIS 584 and MET 363 and van der Waals interactions with seven amino acid residues when compared to standard with three strong hydrogen bond and one van der Waal interactions (Dissanayake et al. 2022).

Conclusion

The performed investigation offers valuable insights into the possible anticancer characteristics of bioactive chemicals obtained from the maritime seagrass species Cymodocea serrulata. The human oestrogen receptor alpha (3ERT), a crucial target in hormone-dependent cancers, was found to have strong binding affinities to the selected compounds, 2-hexadecen-1-ol, n-Nonadecanol-1, Octadecanoic acid ethyl ester, 3,7,11,15-Tetramethyl, n-Hexadecanoic acid and 9,12-Octadecadienoic acid. According to the study's findings, molecular docking is a useful and trustworthy method for locating putative alpha inhibitors of the human oestrogen receptor. This method lays the groundwork for future medication development and optimisation by predicting the binding affinities and patterns of interaction between small compounds and target proteins. The study also investigated the cytotoxic effects of silver nanoparticles on the MCF-7 cells in addition to the molecular docking studies. The results of the cytotoxicity research showed that the nanoparticles had an inhibitory effect. The silver nanoparticles exhibited a minor growth inhibition of 7.02% at a low dosage of 12.5 µg/ml. However, the nanoparticles dramatically suppressed the proliferation of cancer cells by 79.38% at 200 µg/ml. IC50 value was 102.03 µg/ml for the silver nanoparticles, the conventional chemotherapeutic drug doxorubicin showed a higher growth inhibition of 87.65% at a dose of 5 µg/ml. The ability of these compounds to successfully bind to the Human oestrogen receptor alpha, as well as the proven cytotoxicity of silver nanoparticles against breast cancer cells, highlight their potential as viable candidates for the development of novel anticancer therapeutics.

References

- Atashrazm F, Lowenthal RM, Woods GM, Holloway AF, Dickinson JL (2015) Fucoidan and Cancer: A Multifunctional Molecule with Anti-Tumor Potential. Marine Drugs 13(4):2327–2346. https://doi.org/10.3390/md13042327
- Bhuyan PP, Nayak R, Patra S, Abdulabbas HS, Jena M, Pradhan B (2023) Seaweed-Derived Sulfated Polysaccharides; The New Age Chemopreventives: A Comprehensive Review. Cancers 15(3):715. https://doi.org/10.3390/cancers15030715
- Bray F, Ferlay J, Soerjomataram I, Siegel RL, Torre LA, Jemal A (2018) Global cancer statistics 2018: GLOBOCAN estimates of incidence and mortality worldwide for 36 cancers in 185 countries. CA: A Cancer Journal for Clinicians 68(6):394–424. https://doi.org/10.3322/caac.21492
- Chang M-S (2012) Tamoxifen Resistance in Breast Cancer. Biomolecules & Therapeutics 20(3):256–267. https://doi.org/10.4062/biomolther.2012.20.3.256

- Chanthini AB, Balasubramani G, Ramkumar R, Sowmiya R, Balakumaran MD, Kalaichelvan PT, Perumal P (2015) Structural characterization, antioxidant and *in vitro* cytotoxic properties of seagrass, *Cymodocea serrulata* (R.Br.) Asch. & Magnus mediated silver nanoparticles. Journal of Photochemistry and Photobiology B: Biology 153:145–152. https://doi.org/10.1016/j.jphotobiol.2015.09.014
- Das D, Arulkumar A, Paramasivam S, Lopez-Santamarina A, del Carmen Mondragon A, Miranda Lopez JM (2023) Phytochemical Constituents, Antimicrobial Properties and Bioactivity of Marine Red Seaweed (Kappaphycus alvarezii) and Seagrass (Cymodocea serrulata). Foods 12(14):2811. https://doi.org/10.3390/foods12142811
- Datchanamurthy B, Narayanamurthy U, J V S (2022) Preliminary Phytochemical and GC-MS Analysis of Marine Seaweed-Acoathophora deilei (Red alga). Biomedical and Pharmacology Journal 15. https://doi.org/10.13005/bpj/2508
- Atashrazm F, Lowenthal RM, Woods GM, Holloway AF, Dickinson JL (2015) Fucoidan and Cancer: A Multifunctional Molecule with Anti-Tumor Potential. Marine Drugs 13(4):2327–2346. https://doi.org/10.3390/md13042327
- Bhuyan PP, Nayak R, Patra S, Abdulabbas HS, Jena M, Pradhan B (2023) Seaweed-Derived Sulfated Polysaccharides; The New Age Chemopreventives: A Comprehensive Review. Cancers 15(3):715. https://doi.org/10.3390/cancers15030715
- Bray F, Ferlay J, Soerjomataram I, Siegel RL, Torre LA, Jemal A (2018) Global cancer statistics 2018: GLOBOCAN estimates of incidence and mortality worldwide for 36 cancers in 185 countries. CA: A Cancer Journal for Clinicians 68(6):394–424. https://doi.org/10.3322/caac.21492
- Chang M-S (2012) Tamoxifen Resistance in Breast Cancer. Biomolecules & Therapeutics 20(3):256–267. https://doi.org/10.4062/biomolther.2012.20.3.256

- Chanthini AB, Balasubramani G, Ramkumar R, Sowmiya R, Balakumaran MD, Kalaichelvan PT, Perumal P (2015) Structural characterization, antioxidant and *in vitro* cytotoxic properties of seagrass, *Cymodocea serrulata* (R.Br.) Asch. & Magnus mediated silver nanoparticles. Journal of Photochemistry and Photobiology B: Biology 153:145–152. https://doi.org/10.1016/j.jphotobiol.2015.09.014
- Das D, Arulkumar A, Paramasivam S, Lopez-Santamarina A, del Carmen Mondragon A, Miranda Lopez JM (2023) Phytochemical Constituents, Antimicrobial Properties and Bioactivity of Marine Red Seaweed (Kappaphycus alvarezii) and Seagrass (Cymodocea serrulata). Foods 12(14):2811. https://doi.org/10.3390/foods12142811
- Datchanamurthy B, Narayanamurthy U, J V S (2022) Preliminary Phytochemical and GC-MS Analysis of Marine Seaweed-Acoathophora deilei (Red alga). Biomedical and Pharmacology Journal 15. https://doi.org/10.13005/bpj/2508

- Dissanayake IH, Bandaranayake U, Keerthirathna LR, Manawadu C, Silva RM, Mohamed B, Ali R, Peiris DC (2022) Integration of in vitro and in-silico analysis of Caulerpa racemosa against antioxidant, antidiabetic, and anticancer activities. Sci Rep 12(1):20848. https://doi.org/10.1038/s41598-022-24021-y
- Jin J-O, Yadav D, Madhwani K, Puranik N, Chavda V, Song M (2022) Seaweeds in the Oncology Arena: Anti-Cancer Potential of Fucoidan as a Drug—A Review. Molecules 27(18):6032. https://doi.org/10.3390/molecules27186032

- Kim DH, Mahomoodally MF, Sadeer NB, Seok PG, Zengin G, Palaniveloo K, Khalil AA, Rauf A, Rengasamy KR (2021) Nutritional and bioactive potential of seagrasses: A review. South African Journal of Botany 137:216–227. https://doi.org/10.1016/j.sajb.2020.10.018
- Levin ER (2005) Integration of the Extranuclear and Nuclear Actions of Estrogen. Molecular Endocrinology 19(8):1951–1959. https://doi.org/10.1210/me.2004-0390
- Nadar Rajivgandhi G, Chackaravarthi G, Ramachandran G, Kanisha Chelliah C, Maruthupandy M, Alharbi MS, Alharbi NS, Khaled JM, Li W-J (2022) Morphological damage and increased ROS production of biosynthesized silver nanoparticle against MCF-7 breast cancer cells through in vitro approaches. Journal of King Saud University - Science 34(2):101795. https://doi.org/10.1016/j.jksus.2021.101795
- Narayanan M, Chanthini A, Devarajan N, Saravanan M, Sabour A, Alshiekheid M, Chi NTL, Brindhadevi K (2023) Antibacterial and antioxidant efficacy of ethyl acetate extract of *Cymodocea serrulata* and assess the major bioactive components in the extract using GC-MS analysis. Process Biochemistry 124:24–32. https://doi.org/10.1016/j.procbio.2022.10.036
- Rengasamy RRK, Radjassegarin A, Perumal A (2013) Seagrasses as potential source of medicinal food ingredients: Nutritional analysis and multivariate approach. Biomedicine & Preventive Nutrition 3(4):375–380. https://doi.org/10.1016/j.bionut.2013.06.011
- Sanyakamdhorn S, Agudelo D, Bekale L, Tajmir-Riahi HA (2016) Targeted conjugation of breast anticancer drug tamoxifen and its metabolites with synthetic polymers. Colloids and Surfaces B: Biointerfaces 145:55–63. https://doi.org/10.1016/j.colsurfb.2016.04.035
- Senthilkumar K, Manivasagan P, Venkatesan J, Kim S-K (2013) Brown seaweed fucoidan: Biological activity and apoptosis, growth signaling mechanism in cancer. International Journal of Biological Macromolecules 60:366–374. https://doi.org/10.1016/j.ijbiomac.2013.06.030
- Srinivasan K. Sivasubramanian S and Kumaravel S. Phytochemical profiling and GC-MS study of *Adhatoda vasica* leaves. Int.J.Pharm.Bio.Sci, 2013; 5(1):714-720
- Dr.Duke's Phytochemical and Ethno botanical Databases, Phytochemical and Ethnobotanical Databases. www.ars-gov/cgi-bin/duke/. 2013.
- Atkovska, K., Samsonov, S.A., Paszkowski-Rogacz, M. and Pisabarro, M.T. 2014. Multipose binding in molecular docking. Int. J. Mol. Sci. 15, 2622-2645.
- Binkowski TA, Naghibzadeg S and Liang J. (2003) CASTp computed atlas of surface topography of proteins. *Nucleic Acid Res*. 31: 3352– 3355.
- Ghose AK and Crippen GM. (1987)Atomic physicochemical parameters for three dimensional-structure-directed quantitative structure activity relationships. Modelling dispersive and hydrophobic interactions. *J Chem Inf Comput Sci*,27: 21–35.
- Mooers BH. Shortcuts for faster image creation in PyMOL. Protein Sci 2020;29(1):268-76.
- Sahayarayan JJ, Rajan KS, Vidhyavathi R, Nachiappan M, Prabhu D, Alfarraj S, Arokiyaraj S, Daniel AN. In-silico protein-ligand docking studies against the estrogen

protein of breast cancer using pharmacophore based virtual screening approaches. Saudi J Biol Sci. 2021 Jan;28(1):400-407.

- Shruthisrivastava. (2012) evaluation of anti- arthritic potential of the methanolic extract of the aerial parts of costusspeciosus. journal of ayurvedha&integrative medicine, 3(4):
- Trott, O., & Olson, A. J. (2010). AutoDock Vina: Improving the speed and accuracy of docking with a new scoring function, efficient optimization and multithreading. *J. Comput. Chem., 31,* 455–461.
- Velavan, S., Karnan, R., & Kanivalan, N. (2020). A comparative study on *In silico* software's in statistical relation to molecular docking scores. *Asian Journal of Innovative Research, 5*(2), 01-05.
- Vidya SM, Krishna V, Manjunatha BK, Rajesh KP, Bharath BR, Manjunatha H. (2012) Antibacterial and molecular docking studies of entagenic acid, a bioactive principle from seed kernel of Entada pursaetha. DC. *Med Chem Res*,21: 3195-3203.
- Zhang, Y., Lee, P., Liang, S., Zhou, Z., Wu, X., Yang, F., & Liang, H. (2015). Structural basis of non-steroidal anti-inflammatory drug diclofenac binding to human serum albumin. *Chemical biology & drug design*, *86*(5), 1178-1184.